Controlling pathway dynamics of a four-level quantum system with pulse shaping

2016 J. Phys. A: Math. Theor. 49 285302

(http://iopscience.iop.org/1751-8121/49/28/285302)

IOP Publishing Journal of Physics A: Mathematical and Theoretical
J. Phys. A: Math. Theor. **49** (2016) 285302 (13pp) doi:10.1088/1751-8113/49/28/285302

Controlling pathway dynamics of a four-level quantum system with pulse shaping

Dewen Cao[1,2], Ling Yang[1,2], Yaoxiong Wang[1,2], Feng Shuang[1,2,3] and Fang Gao[1]

[1] Institute of Intelligent Machines, Chinese Academy of Sciences, Hefei 230031, People's Republic of China
[2] Department of Automation, University of Science and Technology of China, Hefei, 230026, People's Republic of China
[3] Department of Mechanical Engineering, Anhui Polytechnic University, Wuhu 241000, People's Republic of China

E-mail: gaofang@iim.ac.cn

Received 23 December 2015, revised 8 May 2016
Accepted for publication 20 May 2016
Published 6 June 2016

Abstract

The dynamics of two two-photon absorption (TPA) pathways in a four-level quantum system driven by a laser pulse is investigated in this work. An analytical solution for pulse shaping is proposed to be globally optimal for constructive interference between the two pathways, and accurate spectral boundaries for phase modulation are obtained. The TPA rate can be enhanced by a factor of 8.33 with the optimal pulse instead of the transform limited pulse (TL pulse). Simple control strategies modulating both amplitudes and phases are also designed to increase the TPA amplitude along one pathway while decreasing that along the other simultaneously. The strategies are intuitive and the two pathway amplitudes can differ by two orders of magnitude.

Keywords: two-photon absorption, pathway dynamics, pulse shaping

(Some figures may appear in colour only in the online journal)

1. Introduction

Coherent control is a widely employed way to control quantum dynamics [1–9]. The desired dynamics can be achieved through different quantum pathways, which interfere coherently with each other and can be extracted with the so-called Hamiltonian-encoding and observable-decoding (HE-OD) technique [10–18]. Pathway dynamics in the control of quantum systems becomes more important after HE-OD is proposed to detect and control

the dynamics. In the protocol, the transition amplitude from the initial state $|a\rangle$ to the target state $|b\rangle$ is decomposed into various quantum pathways, which explains details of the control mechanism well. A typical pathway is specified by a sequence of transitions $|a\rangle \rightarrow |l_1\rangle \rightarrow |l_2\rangle \rightarrow \cdots \rightarrow |l_{n-1}\rangle \rightarrow |b\rangle$, where the intermediate states $|l_i\rangle$, $i = 1, 2, \cdots, n-1$, indicate that n steps are involved in this pathway. In the experiment, the encoding is performed with respect to the control field's spectral phases via a standard laser pulse shaper [17, 18], and the desired pathway amplitude is then obtained by decoding the observed signals. HE-OD has been employed to reveal [17] and control [18] pathway dynamics in atomic rubidium vapour.

Different strategies can be employed for pathway control [19, 20]. Generally, in the weak perturbation regime, the two-photon absorption (TPA) process can be effectively controlled by modulating the interference of different photon pairs with frequencies adding up to the final transition energy [21, 22]. Dudovich *et al* [22] proposed an optimal scheme to maximize one TPA pathway amplitude. Lee *et al* [23] explored coherent interference of the two TPA pathways in atomic rubidium both theoretically and experimentally, and their block scheme achieves a rather good effect. In this work, we investigate the coherent control of two TPA pathways in a typical four-level quantum system. The block scheme is modified to achieve the global maximum of the total TPA rate, where the accurate block boundaries are given analytically. Furthermore, four intuitive strategies with both amplitude and phase shaping are proposed to steer the quantum dynamics towards one desired pathway, and the two pathway amplitudes can differ by two orders of magnitude.

The paper is organized as follows. Section 2 introduces the TPA model and the four-level quantum system with two pathways. Section 3 gives the strategies to maximize the constructive interference of the two TPA pathways and manipulate the pathway dynamics. The final conclusions are given in section 4.

2. Theoretical model

According to the second-order perturbation theory, the amplitude of a TPA process induced by a weak laser field $E(t)$ is

$$U(t) = -\sum_n \frac{\mu_{fn}\mu_{ng}}{\hbar^2} \int_{-\infty}^{t} \mathrm{d}t_1 \int_{-\infty}^{t_1} \mathrm{d}t_2 E(t_1) E(t_2) \exp(\mathrm{i}\omega_{fn} t_1) \exp(\mathrm{i}\omega_{ng} t_2) \tag{1}$$

Here μ_{fn} and μ_{ng} are the transition dipoles, $\omega_{ij} = (E_i - E_j)/\hbar$, with $|g\rangle$, $|n\rangle$ and $|f\rangle$ being, respectively, the ground, intermediate and final states, and the summation is performed over all possible intermediate states. Further details of two-photon transition can be found in reference [24]. Usually Fourier synthesis methods are employed in a typical femtosecond pulse shaping experiment [25], where the programmable shaping is performed in the frequency domain with the use of spatial light modulators. Therefore, an equivalent expression in the frequency domain is necessary to understand the process.

With Fourier transformation, the final amplitude after the pulse is over (i.e. $t \rightarrow \infty$) can be written in the frequency domain as a sum of resonant and non-resonant parts [22]:

$$U = -\sum_n U^{(n)} = -\sum_n [U_r^{(n)} + U_{nr}^{(n)}], \tag{2}$$

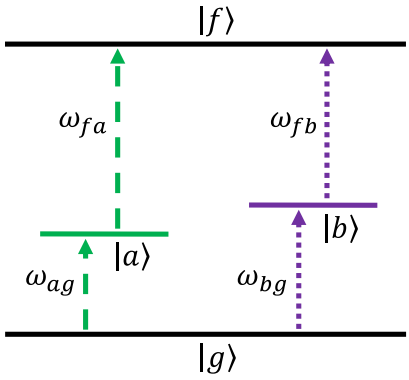

Figure 1. The structure of the four-level quantum system with $\omega_{fn} > \omega_{ng}$, $n = a, b$. The two TPA pathways are labelled with green dashed (pathway $|g\rangle \rightarrow |a\rangle \rightarrow |f\rangle$) and purple dotted (pathway $|g\rangle \rightarrow |b\rangle \rightarrow |f\rangle$) arrows.

with

$$U_r^{(n)} = \frac{\pi \mu_{fn} \mu_{ng}}{\hbar^2} E(\omega_{ng}) E(\omega_{fn}), \tag{3a}$$

$$U_{nr}^{(n)} = \frac{\mu_{fn} \mu_{ng}}{\mathrm{i}\hbar^2} \wp \int_{-\infty}^{\infty} \frac{E(\omega) E(\widehat{\omega})}{\omega_{ng} - \omega} \mathrm{d}\omega, \tag{3b}$$

where $\widehat{\omega} = \omega_{fg} - \omega$, and $\wp$ is the principle value of Cauchy

$$\wp \int_{-\infty}^{\infty} \frac{E(\omega) E(\widehat{\omega})}{\omega_{ng} - \omega} \mathrm{d}\omega = \lim_{\varepsilon \rightarrow 0^+} \left[\int_{-\infty}^{\omega_{ng} - \varepsilon} \frac{E(\omega) E(\widehat{\omega})}{\omega_{ng} - \omega} \mathrm{d}\omega + \int_{\omega_{ng} + \varepsilon}^{\infty} \frac{E(\omega) E(\widehat{\omega})}{\omega_{ng} - \omega} \mathrm{d}\omega \right]. \tag{4}$$

The four-level quantum system to be investigated is shown in figure 1, and there are two TPA pathways $|g\rangle \rightarrow |a\rangle \rightarrow |f\rangle$ and $|g\rangle \rightarrow |b\rangle \rightarrow |f\rangle$. The parameters are $\mu_{ag} = 2.9931$ a.u., $\mu_{fa} = 0.9000$ a.u., $\mu_{bg} = 4.2275$ a.u., $\mu_{fb} = 1.0216$ a.u., $\omega_{ag} = 0.057\,31$ a.u., $\omega_{fa} = 0.059\,79$ a.u., $\omega_{bg} = 0.058\,40$ a.u., and $\omega_{fb} = 0.058\,70$ a.u. These parameters refer to rubidium atoms, and $|g\rangle \rightarrow |a\rangle \rightarrow |f\rangle$ and $|g\rangle \rightarrow |b\rangle \rightarrow |f\rangle$ are just the two TPA pathways reaching the target state $5D_{3/2}$ [16, 19].

A laser pulse with a Gaussian envelope is employed to drive the system from state $|g\rangle$ to state $|f\rangle$ here

$$E(\omega) = B_0 B(\omega) \exp\left\{ -\frac{(\omega - \omega_0)^2}{2\Delta^2} \right\} \mathrm{e}^{\mathrm{i}\phi(\omega)}, \tag{5}$$

where $B_0 = 0.0006$ a.u., small enough to make sure that the light–matter interaction is perturbative, $B(\omega)$ is allowed to vary between 0 and 1 (i.e. $B(\omega) \in [0, 1]$), $\omega_0 = 0.058\,56$ a.u. and $\Delta = 5.7518 \times 10^{-4}$ a.u. Here ω_0 is the center frequency of the pulse spectrum, which is set to $\sim \omega_{fg}/2$. Δ is taken to be large enough to induce a wide spectral width covering all characteristic transition frequencies. The parameters of ω_0 and Δ are the same as in reference [23] and can make the two TPA pathways interfere obviously. $B(\omega)$ is a scaling function, and the corresponding spectral component is blocked when it is equal to zero. $\phi(\omega)$ is the phase function. In section 3, different choices of $B(\omega)$ and $\phi(\omega)$ mark different strategies to maximize the constructive interference of the two TPA pathways and manipulate the pathway dynamics.

For simplicity, the following definitions are adopted

$$\upsilon_n = \frac{\mu_{fn}\mu_{ng}}{\hbar^2}, \tag{6a}$$

$$G(\omega) = \exp\left\{-\frac{(\omega - \omega_0)^2}{2\Delta^2}\right\}, \tag{6b}$$

$$g(\omega) = \exp\left\{-\frac{(\omega - \omega_{fg}/2)^2}{\Delta^2}\right\}, \tag{6c}$$

$$f_n(\omega) = g(\omega)\left(\frac{1}{\omega - \omega_{fn}} + \frac{1}{\omega_{ng} - \omega}\right), \tag{6d}$$

$$f_T(\omega) = \sum_{n=a,b} \upsilon_n f_n(\omega), \tag{6e}$$

$$h(\omega) = B(\omega)B(\widehat{\omega})\mathrm{e}^{\mathrm{i}\phi(\omega)+\mathrm{i}\phi(\widehat{\omega})}. \tag{6f}$$

Since $G(\omega)G(\widehat{\omega}) = g(\omega_0)g(\omega)$, the resonant and non-resonant parts of the n-th pathway can be rewritten as

$$U_r^{(n)} = \pi B_0^2 g(\omega_0)\upsilon_n h(\omega_{fn})g(\omega_{fn}), \tag{7a}$$

$$U_{nr}^{(n)} = -\mathrm{i}B_0^2 g(\omega_0)\upsilon_n \wp\int_{-\infty}^{\infty} \frac{h(\omega)g(\omega)}{\omega_{ng} - \omega}\mathrm{d}\omega. \tag{7b}$$

Here $g(\omega)$ and $h(\omega)$ are axi-symmetric about $\omega = \omega_{fg}/2$, which leads to $g(\widehat{\omega}) = g(\omega)$, and $h(\widehat{\omega}) = h(\omega)$. The Cauchy principle value of $U_{nr}^{(n)}$ can be further simplified by the variable transformation $\omega \to \widehat{\omega}$,

$$\begin{aligned}
&\wp\int_{-\infty}^{\infty} \frac{h(\omega)g(\omega)}{\omega_{ng} - \omega}\mathrm{d}\omega \\
&= \wp\int_{-\infty}^{\omega_{fg}/2} \frac{h(\omega)g(\omega)}{\omega_{ng} - \omega}\mathrm{d}\omega + \int_{\omega_{fg}/2}^{\infty} \frac{h(\omega)g(\omega)}{\omega_{ng} - \omega}\mathrm{d}\omega \\
&= \wp\int_{-\infty}^{\omega_{fg}/2} \frac{h(\widehat{\omega})g(\widehat{\omega})}{\omega_{ng} - \widehat{\omega}}\mathrm{d}\widehat{\omega} + \int_{\omega_{fg}/2}^{\infty} \frac{h(\omega)g(\omega)}{\omega_{ng} - \omega}\mathrm{d}\omega \\
&= \wp\int_{\omega_{fg}/2}^{\infty} \frac{h(\omega)g(\omega)}{\omega - \omega_{fn}}\mathrm{d}\omega + \int_{\omega_{fg}/2}^{\infty} \frac{h(\omega)g(\omega)}{\omega_{ng} - \omega}\mathrm{d}\omega \\
&= \wp\int_{\frac{\omega_{fg}}{2}}^{\infty} h(\omega)f_n(\omega)\mathrm{d}\omega.
\end{aligned} \tag{8}$$

The convergence of the Cauchy principle value is analysed in appendix A. The non-resonant terms of TPA amplitudes can be obtained from equations (A5) and (6*e*)

$$U_{nr}^{(n)} = -\mathrm{i}B_0^2 g(\omega_0)\upsilon_n \int_{\overline{D}_{fn}} h(\omega)f_n(\omega)\mathrm{d}\omega + \mathrm{O}(\delta), \tag{9a}$$

$$U_{nr} = -\mathrm{i}B_0^2 g(\omega_0) \int_{\overline{D}_{fa}\bigcap\overline{D}_{fb}} h(\omega)f_T(\omega)\mathrm{d}\omega + \mathrm{O}(\delta). \tag{9b}$$

Here the region $\overline{D}_{fn} = (\omega_{fg}/2, \omega_{fn} - \delta) \bigcup (\omega_{fn} + \delta, \infty)$, $n = a, b$. (see also in appendix A). In practice, δ is taken to be small enough to ensure the convergence (10^{-9} a.u. in our simulations).

3. Coherent control of two TPA pathways

Different interference of pathways can lead to different dynamics. In this section, the coherent control of the two pathways present in the four-level system will be investigated from two aspects. The first focus is how to maximize the total TPA transition amplitude, and a global optimal solution is proposed. The second is to make one pathway dominate in the TPA process, and four simple intuitive schemes are shown to be effective. Both studies have equations (9*a*) and (9*b*) as the starting point, and the results are shown together in table 1.

3.1. Global optimal scheme for the total TPA transition

Firstly, we define $a' = \upsilon_a(\omega_{fa} - \omega_{ag})$, and $b' = \upsilon_b(\omega_{fb} - \omega_{bg})$. Since $\omega_{fn} > \omega_{ng}$, $f_T(\omega)$ can be written as a fractional form

$$f_T(\omega) = \frac{-(a' + b')g(\omega)(\omega - \omega_{fo})(\omega - \omega_{og})}{(\omega - \omega_{fa})(\omega - \omega_{ag})(\omega - \omega_{fb})(\omega - \omega_{bg})}, \tag{10}$$

where ω_{og} and ω_{fo} are the real roots to make $f_T(\omega) = 0$.

$$\begin{aligned} \omega_{og} &= \frac{\omega_{fg}}{2} - \frac{1}{2}\sqrt{Q}, \\ \omega_{fo} &= \frac{\omega_{fg}}{2} + \frac{1}{2}\sqrt{Q}, \\ Q &= \frac{a'(\omega_{fb} - \omega_{bg})^2 + b'(\omega_{fa} - \omega_{ag})^2}{a' + b'}. \end{aligned} \tag{11}$$

The function $f_T(\omega)$ is plotted versus ω in figure 2(a), where ω_{fo} is between ω_{fb} and ω_{fa}, and ω_{og} is between ω_{ag} and ω_{bg} (not shown).

It is easy to get the following relation about the total TPA amplitude from equations (7*a*) and (9*b*).

$$U = B_0^2 g(\omega_0)\left[\pi \sum_{n=a,b} \upsilon_n h(\omega_{fn}) g(\omega_{fn}) - \mathrm{i}\int_{\overline{D}_{fa}\bigcap\overline{D}_{fb}} h(\omega) f_T(\omega)\mathrm{d}\omega\right] + \mathrm{O}(\delta), \tag{12}$$

$$|U|_{\max} = B_0^2 g(\omega_0)\left[\pi \sum_{n=a,b} \upsilon_n g(\omega_{fn}) + \int_{\overline{D}_{fa}\bigcap\overline{D}_{fb}} |f_T(\omega)|\,\mathrm{d}\omega\right] + \mathrm{O}(\delta). \tag{13}$$

To maximize $|U|$, we have to modulate the combinational phase $\Phi(\omega) = \phi(\omega) + \phi(\widehat{\omega})$ to make all terms of U interfere constructively. Therefore, the equality in equation (13) holds when the phase of the pulse satisfies

$$\Phi(\omega) = \begin{cases} -\frac{\pi}{2} & \left(\frac{\omega_{fg}}{2}, \omega_{fb} - \delta\right) \bigcup (\omega_{fo}, \omega_{fa} - \delta) \\ 0 & D_{fb} \bigcup D_{fa} \\ +\frac{\pi}{2} & (\omega_{fb} + \delta, \omega_{fo}) \bigcup (\omega_{fa} + \delta, \infty), \end{cases} \tag{14}$$

Table 1. Pathway amplitudes with different control schemes. The TL pulse means no pulse shaping (*i.e.* $B(\omega) = 1, \phi(\omega) = 0$). For simplicity, all the values are reduced by a factor of B_0^2. The subscripts r and nr indicate, respectively, the resonant and non-resonant terms of the TPA amplitude, while the superscripts (a) and (b) correspond, respectively, to the two pathways $|g\rangle \rightarrow |a\rangle \rightarrow |f\rangle$ and $|g\rangle \rightarrow |b\rangle \rightarrow |f\rangle$ in figure 1. Lee's scheme [23] and the global optimal scheme aim to maximize the total TPA amplitude $|U|$. Strategies A and B try to make TPA pathway $|g\rangle \rightarrow |a\rangle \rightarrow |f\rangle$ dominate, while strategies C and D are to make pathway $|g\rangle \rightarrow |b\rangle \rightarrow |f\rangle$ dominate.

Terms	$U_r^{(a)}$	$U_{nr}^{(a)}$	$U_r^{(b)}$	$U_{nr}^{(b)}$	U_r	U_{nr}	$U^{(a)}$	$U^{(b)}$	$\|U\|$
TL pulse	3.82	4.95i	12.88	1.57i	16.70	6.52i	3.82+4.95i	12.88+1.57i	17.93
Lee's scheme	3.82	29.67	12.88	101.64	16.70	131.31	33.49	114.52	148.01
Global optimal scheme	3.82	32.52	12.88	100.12	16.70	132.64	36.35	113.00	149.35
Strategy A	3.82	35.70	0.00	1.85	3.82	37.55	39.52	1.85	41.37
Strategy B	3.82	33.47	0.00	−0.95	3.82	32.52	37.29	−0.95	36.34
Strategy C	0.00	−3.66	12.88	102.29	12.88	98.63	−3.66	115.18	111.52
Strategy D	0.00	−1.59	12.88	101.07	12.88	99.48	−1.59	113.95	112.36

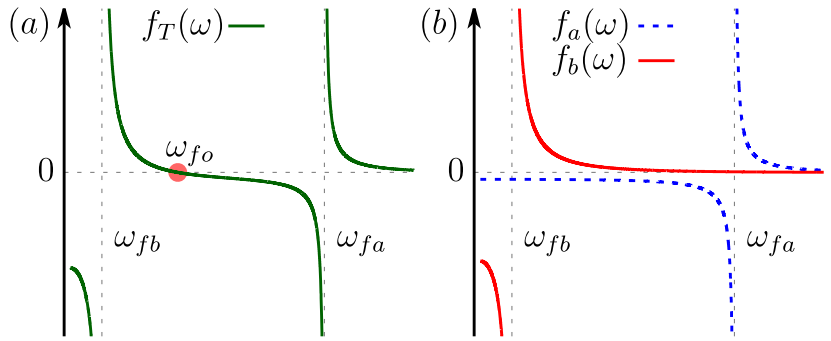

Figure 2. (a) The plot of $f_T(\omega)$ versus ω with $f_T(\omega_{fo}) = 0$. (b) The plots of $f_a(\omega)$ and $f_b(\omega)$ versus ω. In both panels (a) and (b), ω ranges from $\omega_{fg}/2$ to infinity, the same as the integration region in equation (8).

with the region $D_{fn} = (\omega_{fn} - \delta, \omega_{fn} + \delta)$, $n = a, b$. This is just the global optimal scheme for the total TPA amplitude, and the amplitudes $B(\omega)$ are not modulated (i.e. $B(\omega) = 1$).

Lee *et al* [23] have proposed an eight-block scheme to enhance the fluorescence signal of TPA. If the phases of the last four spectral blocks (*i.e.* $\omega > \omega_{fg}/2$) are taken to be zero, their scheme can be expressed as

$$\phi(\omega) = \begin{cases} +\frac{\pi}{2} & (-\infty, \omega_{ag} - \delta) \bigcup (\omega_c, \omega_{bg} - \delta) \\ 0 & D_{ag} \bigcup D_{bg} \bigcup \left(\frac{\omega_{fg}}{2}, \infty\right) \\ -\frac{\pi}{2} & (\omega_{ag} + \delta, \omega_{cg}) \bigcup \left(\omega_{bg} + \delta, \frac{\omega_{fg}}{2}\right). \end{cases} \tag{15}$$

with

$$\omega_{cg} = \frac{v_b\omega_{ag} + v_a\omega_{bg}}{v_a + v_b}, \quad \omega_{fc} = \omega_{fg} - \omega_{cg}. \tag{16}$$

Here the region $D_{ng} = (\omega_{ng} - \delta, \omega_{ng} + \delta)$, $n = a, b$.

Since U just depends on the combinational phase $\Phi(\omega)$, the scheme in equation (15) can be rewritten as

$$\Phi(\omega) = \begin{cases} -\frac{\pi}{2} & \left(\frac{\omega_{fg}}{2}, \omega_{fb} - \delta\right) \bigcup (\omega_{fc}, \omega_{fa} - \delta) \\ 0 & D_{fa} \bigcup D_{fb} \\ +\frac{\pi}{2} & (\omega_{fb} + \delta, \omega_{fc}) \bigcup (\omega_{fa} + \delta, \infty). \end{cases} \tag{17}$$

This is the same as our scheme in equation (14), except that the critical frequency in our scheme is ω_{fo} instead of ω_{fc}. The two schemes are shown in figure 3.

As indicated in table 1, our global optimal scheme can enhance the TPA rate by a factor of 8.33 compared with the TL pulse, which is a little better than Lee's scheme [23]. Our scheme is a global optimal solution to maximize the amplitude $|U|$ by considering exactly its non-resonant terms by a proper variable transformation, while Lee's scheme [23] just takes the dominant non-resonant terms into account when seeking for the spectral boundaries, although it can also achieve a very good outcome.

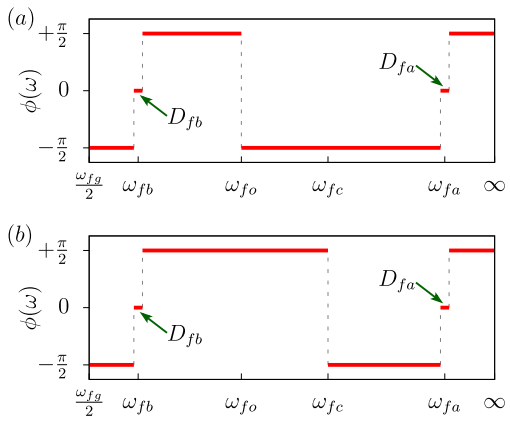

Figure 3. (a) Our global optimal scheme described by equation (14); (b) Lee's scheme described by equation (17). In both schemes, the amplitudes $B(\omega)$ are not modulated (*i.e.* $B(\omega) = 1$), and the phase $\phi(\omega)$ is equal to 0 when $\omega < \omega_{fg}/2$ (not shown).

3.2. Pathway manipulation strategies

In the four-level quantum system, there are two TPA pathways, namely $|g\rangle \rightarrow |a\rangle \rightarrow |f\rangle$ and $|g\rangle \rightarrow |b\rangle \rightarrow |f\rangle$. It is possible to detect and even manipulate pathway amplitudes after the HE-OD technique is proposed and employed in experiments [17, 18]. Here we will try to design simple schemes to manipulate them. To make one pathway dominate in the TPA process, an intuitive strategy is to increase the desired pathway amplitude and decrease the undesired one simultaneously by modulating both amplitudes and phases of the input laser pulse. The plots of $f_a(\omega)$ and $f_b(\omega)$ versus ω are shown in figure 2(b). To increase $|U^{(a)}|$, we can adopt a similar phase shaping scheme as mentioned above, which makes all terms of $U^{(a)}$ interfere constructively. To decrease $|U^{(b)}|$, we can block the spectral region around the resonant frequency ω_{fb}, which makes the resonant term $U_r^{(b)} = 0$, and we can also make the phases of the spectral regions nearby ω_{fb} be the same, which leads to the destructive interference of the dominant components of $U_{nr}^{(b)}$. Without loss of generality, we assume $\phi(\omega) = 0$ and $B(\omega) = 1$ when $\omega \in (-\infty, \omega_{fg}/2)$. The above analysis leads to strategy A which makes pathway $|g\rangle \rightarrow |a\rangle \rightarrow |f\rangle$ dominate,

$$B(\omega) = \begin{cases} 1 & \overline{D}_{fb} \\ 0 & D_{fb}, \end{cases}$$
$$\phi(\omega) = \begin{cases} -\frac{\pi}{2} & \left(\frac{\omega_{fg}}{2}, \omega_{fa} - \delta\right) \\ 0 & D_{fa} \\ +\frac{\pi}{2} & (\omega_{fa} + \delta, \infty). \end{cases} \tag{18}$$

We can also block more spectral regions around ω_{fb} to suppress $U^{(b)}$ more, which leads to strategy B

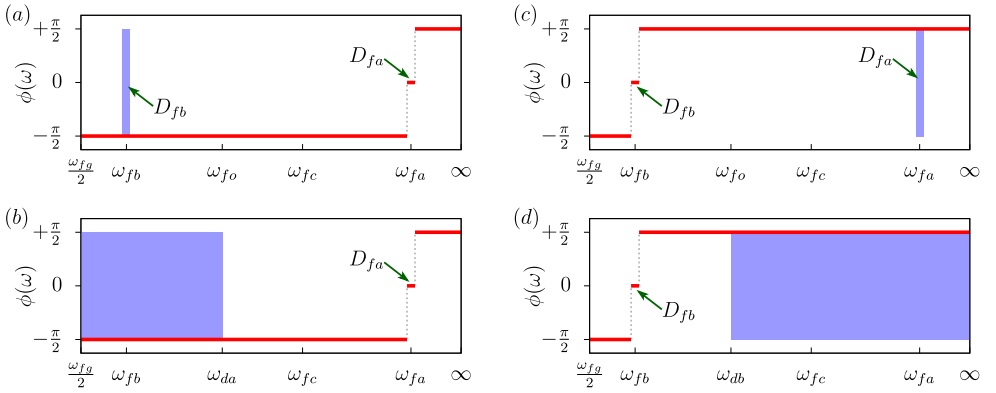

Figure 4. Phases $\phi(\omega)$ and amplitudes $B(\omega)$ of the control pulses in the four pathway manipulation strategies: (a) Strategy *A*; (b) Strategy *B*; (c) Strategy *C*; (d) Strategy *D*. Strategies A and B are to make pathway $|g\rangle \rightarrow |a\rangle \rightarrow |f\rangle$ dominate, while strategies C and D are to make pathway $|g\rangle \rightarrow |b\rangle \rightarrow |f\rangle$ dominate. The phases are all taken to be step functions (indicated by the red solid lines). The amplitudes of the pulses are 0 within the blocked regions (indicated by blue rectangles), and 1 for the other regions. $\phi(\omega)$ is 0 and $B(\omega)$ is 1 when $\omega < \omega_{fg}/2$ (not shown).

$$B(\omega) = \begin{cases} 1 & (\omega_{da}, \infty) \\ 0 & \left(\frac{\omega_{fg}}{2}, \omega_{da}\right), \end{cases}$$
$$\phi(\omega) = \begin{cases} -\frac{\pi}{2} & \left(\frac{\omega_{fg}}{2}, \omega_{fa} - \delta\right) \\ 0 & D_{fa} \\ +\frac{\pi}{2} & (\omega_{fa} + \delta, \infty). \end{cases} \tag{19}$$

where the value of $\omega_{da} \in (\omega_{fb} + \delta, \omega_{fa} - \delta)$ has to be chosen carefully to achieve a better control effect. In practice, it can be obtained by maximizing $|U^{(a)}| - |U^{(b)}|$. The two strategies to make pathway $|g\rangle \rightarrow |a\rangle \rightarrow |f\rangle$ dominate are shown in figures 4(a) and (b), respectively.

Similarly, strategies *C* (described by equation (20)) and *D* (described by equation (21)) can be designed to make pathway $|g\rangle \rightarrow |b\rangle \rightarrow |f\rangle$ dominate

$$B(\omega) = \begin{cases} 1 & \overline{D}_{fa} \\ 0 & D_{fa}, \end{cases}$$
$$\phi(\omega) = \begin{cases} -\frac{\pi}{2} & \left(\frac{\omega_{fg}}{2}, \omega_{fb} - \delta\right) \\ 0 & D_{fb} \\ +\frac{\pi}{2} & (\omega_{fb} + \delta, \infty). \end{cases} \tag{20}$$

$$B(\omega) = \begin{cases} 1 & \left(\frac{\omega_{fg}}{2}, \omega_{db}\right) \\ 0 & (\omega_{db}, \infty), \end{cases}$$
$$\phi(\omega) = \begin{cases} -\frac{\pi}{2} & \left(\frac{\omega_{fg}}{2}, \omega_{fb} - \delta\right) \\ 0 & D_{fb} \\ +\frac{\pi}{2} & (\omega_{fb} + \delta, \infty). \end{cases} \tag{21}$$

Here a suitable value $\omega_{db} \in (\omega_{fb} + \delta, \omega_{fa} - \delta)$ is also necessary in strategy D. It can also be obtained by maximizing $|U^{(b)}| - |U^{(a)}|$. The two strategies C and D are shown in figures 4(c) and (d) respectively.

As seen in table 1, strategies A and B can both eliminate the resonant term $U_r^{(b)}$ by blocking specific spectral regions, and greatly suppress the non-resonant term $U_{nr}^{(b)}$ via destructive interference. In the mean time, the amplitudes of $U_r^{(a)}$ and $U_{nr}^{(a)}$ are approximately as large as those in Lee's scheme [23] and our global optimal scheme. Strategy B attempts to block more regions near ω_{fb}, and thus $U_{nr}^{(b)}$ is suppressed more, which leads to the larger ratio of $U^{(a)}$ to $U^{(b)}$ although the magnitude of $U^{(a)}$ is smaller than that in strategy A. In other words, there exists a balance between enhancement of $|U_{nr}^{(a)}|$ and suppression of $|U_{nr}^{(b)}|$. Similar behaviour is observed in strategies C and D. In all strategies, the TPA amplitudes of the desired and undesired pathways in the four strategies can differ by two orders of magnitude, which indicates that the pathway dynamics can be manipulated effectively.

4. Concluding remarks

The coherent control of pathway dynamics in a four-level quantum system is investigated in this work. A global optimal scheme is proposed to maximize the magnitude of the total TPA rate. With accurate spectral boundaries for phase modulation, the constructive interference between the two TPA pathways is maximized. The manipulation of the two TPA pathways is achieved by some simple intuitive schemes, where the spectral bands around the resonant frequencies of the undesired pathway are blocked and constructive interference of the non-resonant terms of the desired pathway is induced by phase shaping. The simulation results show that the strategies are effective for pathway manipulation, that is, enhancing one pathway amplitude and suppressing the other simultaneously.

This paper only investigates a two-pathway quantum system with special energy structure (i.e. $\omega_{ag}, \omega_{bg} < \omega_{fg}/2$). As seen in equation (11), there are two real roots for $f_T(\omega) = 0$ when ω_{ag} and ω_{bg} are both larger or smaller than $\omega_{fg}/2$. The spectral boundaries for pulse shaping could be changed when imaginary roots appear for other cases (*i.e.* $\omega_{ag} < \omega_{fg}/2 < \omega_{bg}$), which needs to be carefully studied. Furthermore, the complexity increases for more general N-pathway ($N > 2$) quantum systems. How to generalize our schemes will be explored in future work.

Acknowledgments

This work is supported by the National Natural Science Foundation of China (Grants No. 61203061, No. 61403362, 61374091, and No. 61473199). F Shuang thanks the Leader talent plan of the Universities in Anhui Province for their support.

Appendix A. Convergence analysis of the Cauchy principle value

The Cauchy principle value in equation (8) equates to an integral over region $(\omega_{fg}/2, \infty)$, which can be further divided into two regions $D_{fn} = (\omega_{fn} - \delta, \omega_{fn} + \delta)$ and $\overline{D}_{fn} = (\omega_{fg}/2, \infty) - D_{fn}$ ($n \in \{a, b\}$). In the following, we will prove that the integral over the region D_{fn} is of the order of $O(\delta)$ and thus the principle value converges to the integral over the region $\overline{D}_{fn}$ when δ is small enough.

For the two integral kernels in equation (8), we have

$$\begin{aligned}
&\left|\wp\int_{D_{fn}}\frac{g(\omega)}{\omega-\omega_{fn}}\mathrm{d}\omega\right| \\
&=\left|\lim_{\varepsilon\to0^+}\left[\int_{\omega_{fn}-\delta}^{\omega_{fn}-\varepsilon}\frac{g(\omega)}{\omega-\omega_{fn}}\mathrm{d}\omega+\int_{\omega_{fn}+\varepsilon}^{\omega_{fn}+\delta}\frac{g(\omega)}{\omega-\omega_{fn}}\mathrm{d}\omega\right]\right| \\
&=\left|\lim_{\varepsilon\to0^+}\left[\int_{-\frac{\delta}{\Delta}}^{-\frac{\varepsilon}{\Delta}}\frac{g(\omega_{fn}+\Delta x)}{x}\mathrm{d}x+\int_{\frac{\varepsilon}{\Delta}}^{\frac{\delta}{\Delta}}\frac{g(\omega_{fn}+\Delta x)}{x}\mathrm{d}x\right]\right| \\
&=\left|\lim_{\varepsilon\to0^+}\left[\int_{\frac{\varepsilon}{\Delta}}^{\frac{\delta}{\Delta}}\frac{g(\omega_{fn}+\Delta x)-g(\omega_{fn}-\Delta x)}{x}\mathrm{d}x\right]\right| \\
&=\left|\lim_{\varepsilon\to0^+}\left[\int_{\frac{\varepsilon}{\Delta}}^{\frac{\delta}{\Delta}}g(\omega_{fn}+\Delta x)\frac{1-\exp\left\{\frac{4x(\omega_{fn}-\omega_{fg}/2)}{\Delta}\right\}}{x}\mathrm{d}x\right]\right| \\
&<g(\omega_{fn})\lim_{\varepsilon\to0^+}\int_{\varepsilon/\Delta}^{\delta/\Delta}\frac{\exp\left\{\frac{4x(\omega_{fn}-\omega_{fg}/2)}{\Delta}\right\}-1}{x}\mathrm{d}x.
\end{aligned}\tag{A1}$$

and

$$\begin{aligned}
&\left|\int_{D_{fn}}\frac{g(\omega)}{\omega_{ng}-\omega}\mathrm{d}\omega\right| \\
&=\int_{\omega_{fn}-\delta}^{\omega_{fn}+\delta}\frac{g(\omega)}{\omega-\omega_{ng}}\mathrm{d}\omega<\frac{2\delta g(\omega_{fn}-\delta)}{\omega_{fn}-\delta-\omega_{ng}} \\
&\approx\frac{2\delta g(\omega_{fn})}{\omega_{fn}-\omega_{ng}}=\mathrm{O}(\delta).
\end{aligned}\tag{A2}$$

With the expansion $e^x=\sum_{n=0}^{\infty}\frac{x^n}{n!}$, equation (A1) becomes

$$\begin{aligned}
&\left|\wp\int_{D_{fn}}\frac{g(\omega)}{\omega-\omega_{fn}}\mathrm{d}\omega\right| \\
&<g(\omega_{fn})\sum_{n=1}^{\infty}\frac{\left(\frac{4\delta(\omega_{fn}-\omega_{fg}/2)}{\Delta^2}\right)^n}{n!} \\
&=g(\omega_{fn})\left[\exp\left\{\frac{4\delta(\omega_{fn}-\omega_{fg}/2)}{\Delta^2}\right\}-1\right] \\
&=g(\omega_{fn})\left\{\frac{4\delta(\omega_{fn}-\omega_{fg}/2)}{\Delta^2}+\mathrm{O}(\delta^2)\right\}=\mathrm{O}(\delta)
\end{aligned}\tag{A3}$$

Due to the limitation of spectral resolution in experiment, the spectral phases and amplitudes could be considered the same within D_{fn} if δ is small enough. Without loss of generality, it is assumed that $h(\omega)=h(\omega_{fn})$ when $\omega\in D_{fn}$.

Since $|h(\omega)| \leqslant 1$, we have

$$\begin{aligned}
&\wp\int_{D_{fn}} h(\omega) f_n(\omega)\mathrm{d}\omega \\
&= \wp\int_{D_{fn}} h(\omega_{fn}) g(\omega)\left(\frac{1}{\omega - \omega_{fn}} + \frac{1}{\omega_{ng} - \omega}\right)\mathrm{d}\omega \\
&\leqslant \left|\int_{D_{fn}} \frac{g(\omega)}{\omega_{ng} - \omega}\mathrm{d}\omega\right| + \left|\wp\int_{D_{fn}} \frac{g(\omega)}{\omega - \omega_{fn}}\mathrm{d}\omega\right| \\
&= \mathrm{O}(\delta). \qquad \text{(A4)}
\end{aligned}$$

So we arrive at the conclusion

$$\wp\int_{-\infty}^{\infty} \frac{h(\omega) g(\omega)}{\omega_{ng} - \omega}\mathrm{d}\omega = \int_{\overline{D}_{fn}} h(\omega) f_n(\omega)\mathrm{d}\omega + \mathrm{O}(\delta) \qquad \text{(A5)}$$

References

[1] Meshulach D and Silberberg Y 1998 Coherent quantum control of two-photon transitions by a femtosecond laser pulse *Nature* **396** 239–42

[2] Ideguchi T, Yoshioka K, Mysyrowicz A and Kuwata-Gonokami M 2008 Coherent quantum control of excitons at ultracold and high density in cu_2O with phase manipulated pulses *Phys. Rev. Lett.* **100** 233001

[3] Silberberg Y 2009 Quantum coherent control for nonlinear spectroscopy and microscopy *Ann. Rev. Phys. Chem.* **60** 277–92

[4] Herek J L, Wohlleben W, Cogdell R J, Zeidler D and Motzkus M 2002 Quantum control of energy flow in light harvesting *Nature* **417** 533–5

[5] Flissikowski T, Betke A, Akimov I A and Henneberger F 2004 Two-photon coherent control of a single quantum dot *Phys. Rev. Lett.* **92** 227401

[6] Nelson R J, Weinstein Y, Cory D and Lloyd S 2000 Experimental demonstration of fully coherent quantum feedback *Phys. Rev. Lett.* **85** 3045–8

[7] Boutu W *et al* 2008 Coherent control of attosecond emission from aligned molecules *Nat. Phys.* **4** 545–9

[8] Petersen I R 2011 Cascade cavity realization for a class of complex transfer functions arising in coherent quantum feedback control *Automatica* **47** 1757–63

[9] Zhang J, Wu R B, Liu Y x, Li C W and Tarn T J 2012 Quantum coherent nonlinear feedback with applications to quantum optics on chip *IEEE Trans. Autom. Control* **57** 1997–2008

[10] Mitra A and Rabitz H 2003 Identifying mechanisms in the control of quantum dynamics through hamiltonian encoding *Phys. Rev.* A **67** 033407

[11] Mitra A, Solá I R and Rabitz H 2003 Revealing quantum-control mechanisms through hamiltonian encoding in different representations *Phys. Rev.* A **67** 043409

[12] Mitra A and Rabitz H 2006 Quantum control mechanism analysis through field based hamiltonian encoding *J. Chem. Phys.* **125** 194107

[13] Mitra A and Rabitz H 2008 Quantum control mechanism analysis through field based hamiltonian encoding: a laboratory implementable algorithm *J. Chem. Phys.* **128** 044112

[14] Mitra A, Sola I R and Rabitz H 2008 Understanding the role of respresentation in controlled quantum-dynamical mechanism analysis *Phys. Rev.* A **77** 043415

[15] de Castro R R and Rabitz H 2010 Laboratory implementation of quantum-control-mechanism identification through hamiltonian encoding and observable decoding *Phys. Rev.* A **81** 063422

[16] Gao F, Rey-de Castro R, Donovan A M, Xu J, Wang Y, Rabitz H and Shuang F 2014 Pathway dynamics in the optimal quantum control of rubidium: Cooperation and competition *Phys. Rev.* A **89** 023416

[17] de Castro R R, Cabrera R, Bondar D I and Rabitz H 2013 Time-resolved quantum process tomography using hamiltonian-encoding and observable-decoding *New J. Phys.* **15** 025032

[18] Rey-de Castro R, Leghtas Z and Rabitz H 2013 Manipulating quantum pathways on the fly *Phys. Rev. Lett.* **110** 223601
[19] Gao F, Wang Y, Rey-de Castro R, Rabitz H and Shuang F 2015 Quantum control and pathway manipulation in rubidium *Phys. Rev.* A **92** 033423
[20] Fang G, Yao-xiong W, De-wen C and Feng S 2015 Coherent control of multiple 2nd-order quantum pathways *Chinese J. Chem. Phys.* **28** 426–30
[21] Meshulach D and Silberberg Y 1999 Coherent quantum control of multiphoton transitions by shaped ultrashort optical pulses *Phys. Rev.* A **60** 1287–92
[22] Dudovich N, Dayan B, Faeder S M G and Silberberg Y 2001 Transform-limited pulses are not optimal for resonant multiphoton transitions *Phys. Rev. Lett.* **86** 47–50
[23] Lee H-g, Kim H, Lim J and Ahn J 2013 Quantum interference control of a four-level diamond-configuration quantum system *Phys. Rev.* A **88** 053427
[24] Faisal F H M 1987 *Theory of Multiphoton Processes* (New York: Springer) ch 2
[25] Weiner A M 2000 Femtosecond pulse shaping using spatial light modulators *Rev. Sci. Instrum.* **71** 1929–60